Tissue distribution, metabolism, and elimination of Victoria Pure Blue BO in rainbow trout: Main metabolite as an appropriate residue marker

Estelle Dubreil-Cheneau, Michel Laurentie, Jean-Michel Delmas, Morgane Danion, Thierry Morin, Dominique Hurtaud-Pessel, Alexis Viel, Pascal Sanders, Eric Verdon

Tissue distribution, metabolism, and elimination of Victoria Pure Blue BO in rainbow trout: main metabolite as an appropriate residue marker

Estelle Dubreil[a*], Michel Laurentie[a], Jean-Michel Delmas[a], Morgane Danion[b], Thierry Morin[b], Dominique Hurtaud-Pessel[a], Alexis Viel[a], Pascal Sanders[a] and Eric Verdon[a]

[a] Laboratory of Fougères, French Agency for Food, Environmental and Occupational Health & Safety, ANSES, Fougères, France.
[b] Laboratory of Ploufragan-Plouzané-Niort, French Agency for Food, Environmental and Occupational Health & Safety, ANSES, Ploufragan-Plouzané-Niort, France.

*Corresponding author. Tel.: 33(2)-99-17-27-54

E-mail address: estelle.dubreil@anses.fr

Keywords: mass spectrometry, fish metabolism, dyes, treatment, depuration, kinetics

Highlights

- The metabolism of Victoria Pure Blue BO (VPBO) was investigated in rainbow trout.
- Residues were detected by LC-HRMS in muscle, plasma, skin, and liver.
- The half-lives of VPBO and the main metabolite were assessed.
- Deethyl-leuco-VPBO is proposed as a marker of exposure to VPBO in rainbow trout.

Graphical abstract

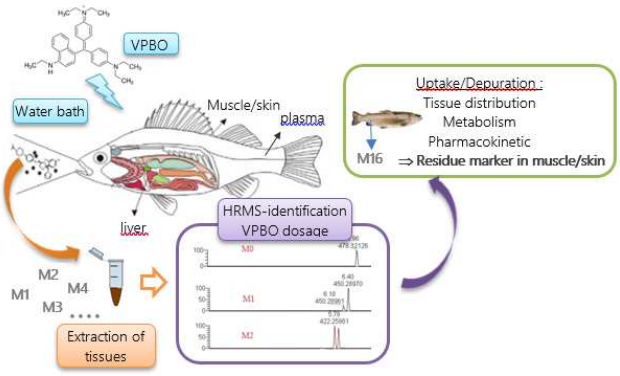

Abstract

Victoria Pure Blue BO is a dye that bears some therapeutic activity and that can be retrieved in effluent or may be used in aquaculture as a prohibited drug. In this study, the metabolism and tissue distribution during uptake and

depuration of VPBO were investigated in order to propose a residue marker of illegal treatment in fish. The dye was administered to rainbow trout (*oncorhynchus mykiss*) for one day by water bath at a dose of 0.1 $mg.L^{-1}$. The concentrations of VPBO in all tissues increased rapidly during the treatment period, reaching a C_{max} of 567 ± 301 $\mu g.L^{-1}$ in plasma and 1,846 $\mu g.kg^{-1}$ ±517 for liver after two hours. After placing the rainbow trout in a clean water bath for a 64 day-period of depuration, the concentrations in the tissues and plasma decreased to reach comparable levels for muscle and for skin after 33 days. The concentrations measured were still above the LOQ at 2.26 ± 0.48 $\mu g.kg^{-1}$ for muscle and 2.85 ± 1.99 $\mu g.kg^{-1}$ for skin at the end of the depuration period. The results indicated the existence of 14 phase I metabolites and one glucuronide conjugated metabolite. Non-compartmental analysis was applied to assess the pharmacokinetic parameters. The half-life in edible muscle of the main metabolite detected, deethyl-leuco-VPBO, was found to be 22.5 days compared to a half-life of 19.7 days for the parent VPBO. This study provides new information to predict a VPBO drug treatment of aquacultured species via a proposed new residue marker.

1. Introduction

Victoria Pure Blue BO (VPBO), also known as Basic blue 7, is a dye that was found in contaminated panga fish (*pangasius bocourti*) imported from Vietnam in 2010. The contamination was reported in Europe via the Rapid Alert System for Food and Feed (RASFF) managed by the European Union (notification 2010.1372) (RASFF-portal, European Commission). The contamination could have originated from environmental effluent waste because Basic blue 7 is commonly used in the industry to dye certain textiles (Gessner and Mayer, 2000). Alternatively, it could have come from intentional and illegal treatment in aquaculture. The efficacy of the substance has not been proven in aquaculture, but it has been demonstrated in the past that it could bear some therapeutic activity. A research team (Alderman, 1982) developed *in vitro* tests to determine the efficacy of 11 therapeutic triarylmethane dyes, including VPBO, against the parasitic fungi *Saprolegnia parasitica* in fish. In a recent report issued by the European Food Safety Authority (EFSA), VPBO was classified as potentially genotoxic, along with 19 other dyes, due to a lack of knowledge regarding its genotoxicity (ECHA; EFSA et al., 2017). VPBO has been found to efficiently bind to DNA and to mediate its photochemical destruction in tumor cells (Lewis and Indig, 2001, 2002). Based on this isolated information and modeling using a quantitative structure-activity relationship (QSAR) approach, EFSA concluded that VPBO should be considered genotoxic (EFSA et al., 2017). The dye was assigned to group I on the basis of a decision tree applying a toxicological screening value (TSV) of

61 0.0025 µg.kg^{-1} body weight per day (EFSA et al., 2017). This TSV could serve as a basis in the near future if
62 EFSA sets a Reference Point for Action (RPA), an action limit related to illegal veterinary drugs found in animal
63 food products. The suspicion of toxicity was recently underpinned by a study within the framework of the Tox21
64 national program in the United States. The toxicity of 10,000 chemicals has been studied in 70 different cell tests
65 covering more than 200 cells signaling pathways. While MG is ranked among the 30 most active drugs, VPBO
66 (basic blue 7) is the most active compound among environmental contaminants (Ngan et al., 2019). In addition,
67 the structure of VPBO, a cationic dye derived from the family of triarylmethanes by the replacement of an aryl
68 group and methyl groups by a naphtyl group and ethyl groups, respectively, may result in certain physicochemical
69 properties associated to the well-known compounds Malachite Green (MG) and Crystal Violet (CV). Probably the
70 most widely used of these chemicals is MG, which is the most popular fungicide in farmed and pet fish and is also
71 effective against ectoparasites in certain protozoan parasite conditions (Alderman, 1985; Srivastava et al., 2004).
72 Since MG and its major metabolite Leuco-Malachite Green (LMG) have several toxic effects in mammalian cells,
73 MG has never been registered as a veterinary medicinal product in the European Union; this is also the case for
74 Crystal Violet. The United States Food and Drug Administration has also not approved any use of these dyes (Culp
75 et al., 1999; Srivastava et al., 2004; Verdon et al., 2015). Despite their toxicity in humans and fish, MG and CV
76 are still used worldwide, probably because no other pharmaceutical drugs have proven to be as effective, and too
77 few therapeutic treatments are currently approved in fish farming (Schnick, 1988; Sudova et al., 2007; Okocha et
78 al., 2018). It has been found that illegal drugs are sometimes replaced by similar illegal drugs or cocktails of these
79 substances (Dervilly-Pinel et al., 2015; Gallart-Ayala et al., 2015).
80 Although LMG is the main residue marker of MG illegal treatment in aquaculture practices, no residue marker has
81 ever been defined for the Victoria dye family and in particular, for VPBO. A previous *in vitro* study in rainbow
82 trout involving incubation of subcellular fractions with dyes suggested that the main metabolite would be deethyl-
83 VPBO (Dubreil et al., 2020b). A previous *in vivo* metabolomics study in treated rainbow trout led to the discovery
84 of certain endogenous bile acid markers and also two VPBO metabolites (Dubreil et al., 2019b, 2020a). To the
85 best of our knowledge, no pharmacokinetic study has ever been carried out on the VPBO compound in fish.
86 However, a few studies described the pharmacokinetics of MG and LMG. MG is rapidly absorbed in different fish
87 species, partly depending on the pH and water temperature in ponds, and it is reduced to its leucoform (LMG) that
88 remains in tissues for long periods (Alderman and Clifton-Hadley, 1993; Máchová et al., 1996; Plakas et al., 1996;
89 Bergwerff et al., 2004; Jiang et al., 2009; Bajc et al., 2011; Kwan et al., 2020).

In order to provide information for food control, the present study was performed in rainbow trout to determine the appropriate residue marker after waterborne exposure to VPBO. The objectives were (1) to identify the main metabolite of VPBO in treated rainbow trout; (2) to characterize the tissue distribution of VPBO and its main metabolite found in treated rainbow trout during the uptake and depuration periods; (3) to estimate and compare the half-lives of VPBO and its major metabolite in muscle and skin; and (4) to suggest a residue marker in edible tissue (muscle + skin) for appropriate food safety assessments.

2. Materials and methods

2.1. Reagents and analytical standards

The standard substances Victoria Pure Blue BO (VPBO), and internal standard (IS) Malachite Green-d_5 (MG-d_5), were purchased from Sigma-Aldrich (Europe). The IS Crystal Violet-d_6 (CV-d_6) was obtained from WITEGA (Berlin, Germany). MG-d_5 was used to correct the peak area of MG and CV-d_6 for VPBO. For the analytical assay, a stock solution of VPBO was prepared at 100 $\mu g.mL^{-1}$ in methanol (not dedicated to the animal study). Stock solutions were further diluted to obtain several concentrations ranging from 0.01 $\mu g.mL^{-1}$ to 1 $\mu g.mL^{-1}$. The internal standards were prepared at 0.1 $mg.mL^{-1}$ in acetonitrile. For the rainbow trout experiment, a stock solution of VPBO was prepared at 1000 $\mu g.mL^{-1}$ in water.

Acetonitrile, methanol, ammonium acetate, and formic acid were of the appropriate analytical grade (HPLC grade). Water was purified using a Milli-Q system (Millipore, Taunton, MA, USA).

2.2. Experimental study design

This study was conducted in order to evaluate the uptake and depuration kinetics of the parent compound and its major metabolites.

A total of 100 specific pathogen-free rainbow trout including a mixture of males and females from the same genetic group were used in this experiment. They were handled at the protected and monitoring facilities of the ANSES Plouzané laboratory site (France). The fishes in the study batch were one year old, with a weight of 105 ± 25 g and length of 15 ± 2 cm. They were fed with commercial dry pellets at 1.5 % body weight (Neo Prima 4, Le Gouessant Aquaculture, France) once a day.

The experimental tank of 400 L was maintained in an open circuit with purified fresh river water at a flow rate of 0.3 $m^3.h^{-1}$ (temperature 13±1°C, dissolved oxygen < 90%, pH close to 8, and free of nitrates and nitrites)

120 throughout the experiment. The tank was maintained in a natural light/dark cycle (14h/10h in spring,
121 approximately) in a room with an air volume change every hour.
122 After one week in acclimation, 20 control fishes free of exposure were collected and euthanized to obtain blank
123 matrices. The system was then positioned in a closed-circuit configuration where the tank was exposed to 0.1
124 $mg.L^{-1}$ of VPBO by adding 40 mL of a standard solution dissolved in water at 1 $g.L^{-1}$ into the tank (dose of 40
125 $mg.kg^{-1}$ b.w. of VPBO). After a 24-hour accumulation period, the fishes were transferred to a new tank, for a 64-
126 day depuration period in a purified fresh river water open circuit.
127 Six fishes were randomly sampled at several sampling dates:
128 - during the 24-hour exposure period at: 0.083, 0.25, 0.417 and 1 day.
129 - post treatment during the depuration period at 2, 3, 5, 9, 17, 34, 49 and 65 days.
130 For each fish, 1 mL of blood was withdrawn from the caudal vein by means of a lithium heparinized vacutainer
131 (BD Vacutainer LH 85 IU). Whole blood samples were centrifuged (1,200 x *g*, 10 min, 4°C) and plasma was
132 stored at -80°C. Fishes were euthanized after collecting blood by percussive stunning with a head blow, and were
133 then measured and weighed. Liver and muscles with skin were removed and stored at -80°C for future analysis.
134 Skin was separated from muscle before freezing. The European Medicines Agency (EMA) has indicated that the
135 target tissue considered appropriate for Salmonidae is muscle including the skin, in natural proportions, as the
136 edible tissue in fish. However, for the purposes of food safety assessments for prohibited drugs, it was decided to
137 separate muscle and skin to have a clear picture of contamination in individual tissues (CVMP, 1998).
138 This study was approved by the French Ethics Committee No.16, reference number 12222-201711161618463.
139

140 **2.3. Sample preparation for the study of VPBO in muscle, plasma, skin, and liver**

141 Samples were weighed (2 g of mixed muscle, 200 µL of plasma, 200 mg of mixed skin, 200 mg of mixed liver)
142 and transferred to a centrifuge tube. Then 100 µL for muscle or 10 µL for plasma, skin, and liver of the internal
143 standard solutions (MG-d_5 and CV-d_6 at 50 $\mu g.L^{-1}$ in acetonitrile) were added. The sample was vortex-mixed and
144 left to stand for 10 minutes in the dark. Then, acetonitrile was added: 8 mL for muscle, 1 mL for plasma, skin, and
145 liver). The sample was vortex-mixed to homogenize the material with the solvent. The sample was further placed
146 on a mechanical rotary shaker for 15 minutes at 100 rpm, and then placed in an ultrasound bath for 5 min at 20°C
147 ±2°C. Samples were centrifuged for 10 min at 20,000 x *g* refrigerated at 4°C. The supernatant was transferred to
148 a polypropylene tube and evaporated to dryness under gentle nitrogen flow at 50°C. The dry extracts was dissolved
149 by ultrasound in acetonitrile/water for reconstitution (80/20, v/v) (500 µL for muscle, 200 µL for plasma, skin, and

liver), and vortex-mixed. The residue for muscle was extracted through a 0.45 µm syringe PVDF filter, and the residues for the other matrices were extracted by centrifugation for 5 min at 20,000 x *g* refrigerated at +4°C. The samples were transferred to LC vials.

2.4. Liquid chromatography-high resolution mass spectrometry analysis

The investigation of metabolism was conducted in two steps: first the concentration of the parent compound was measured via a quantitative LC-HRMS method, and then the formation of metabolites was studied via the metabolite research software MetWorks®. Chromatography was performed on a Thermofisher U-HPLC Accela system (Bremen, Germany), fitted with a Phenomenex Luna C18 (2) column (Phenomenex, Torrance, CA, USA) (150 × 2.0 mm, 3 µm). The final reconstitution solution for samples after extraction was prepared by mixing 80% acetonitrile with 20% water. Chromatographic separation was carried out using two mobile phase preparations, consisting of mobile phase (A), a mixture of ammonium acetate 10 $mM.L^{-1}$ and 0.1% formic acid, and mobile phase (B), 100% acetonitrile. The gradient conditions were as follows: from 0 to 4 min, ramp up linearly from 98 to 2% of mobile phase A and hold for 4 min, then ramp back over 0.1 min to initial conditions and hold for 4 min to re-equilibrate the system. The flow rate was set at 0.2 $mL.min^{-1}$, the injection volume was 10 µL, and the column oven was maintained at 25°C. The LTQ Orbitrap XL mass spectrometer (Thermofisher, Bremen, Germany) was operated with an electrospray ionization probe in positive mode, using the following source parameters: sheath gas flow rate: 30 arb; auxiliary gas flow rate: 10 arb; sweep gas flow rate: 2 arb; ion spray voltage: 5 kV; capillary temperature: 275°C; capillary voltage: 35 V; and tube lens: 90 V. The instrument was calibrated using the manufacturer's calibration solution, to reach mass accuracies in the 1-3 ppm range. The instrument was operated in full-scan mode from m/z 100-1,000, at a resolving power of 60,000 (full width at half maximum), allowing VPBO detection as $VPBO^+$ ions, as well as metabolite formation investigations using the metabolism software MetWorks 1.3.0. SP1 (Thermo Fisher Scientific, Waltham, MA, USA). Exact masses of the peaks detected by this software were extracted with a mass window of 5 ppm around the ionized precursor ion, to confirm or discard their identity. For confirmation of the identity of the major metabolite (deethyl-leuco-VPBO), MS^2 mass fragmentation of the compound was performed in the LTQ-Orbitrap mass analyser. The energy for collision-induced dissociation (CID) were set at 35 eV and 70 eV, with an isolation width of *m/z* 1.

2.5. Validation of the analytical method for VPBO

Calibration curves were prepared by spiking muscle, plasma, skin, and liver prior extraction with VPBO, with the following concentrations: 0.5, 1, 5, 10, and 50 µg.kg^{-1}. These calibration samples were prepared and analyzed in duplicate on three different days for muscle, and 1 day each for plasma, skin, and liver to combine the three series. This protocol was chosen in order to select the most appropriate response function. The validation standards were reconstituted samples with matrix containing known concentrations of the analyte of interest. These were prepared at three levels of concentration corresponding to low (estimated limit of quantification), intermediate, and high concentrations levels: 0.5, 5 and 50 µg.kg^{-1} of VPBO. These validation samples were prepared and analyzed in triplicate on three consecutive days for muscle, and 1 day each for plasma, skin, and liver to combine the three series of the three days.

The statistical analysis of validation data was based on the accuracy profile using e.noval® software, Version 4.1 b (Pharmalex, Liège, Belgium). The concentrations of the validation samples were calculated from the experimental result to determine mean relative bias, repeatability, intermediate precision, and β-expectation tolerance interval limits with a 90% level. The acceptance limit was set at ± 50%.

2.6. Pharmacokinetic analysis

For the dosing during treatment and depuration periods, concentrations under the lower limit of quantification (LOQ) were discarded. Samples above the upper LOQ were diluted to enter into the validated range. Matrix-matched calibration curves were performed for the dosing of VPBO in several batches. The equation of the curves from VPBO dosing were used to assess the concentration of DLVPBO, assuming the mass spectrometric response would be equivalent, because no specific analytical standard is commercially available for this metabolite.

A non-compartmental model was used to determine the pharmacokinetic parameters. All pharmacokinetic analyses were performed with Phoenix WinNonlin 8.2 software (Certara, Saint Louis, MO, USA).

2.6.1. Non-Compartmental Analysis

The observed data were sparse; one point per animal and six animals per time point were used. In this type of design, it was not possible to distinguish inter-individual from intra-individual variability, and consequently the present analysis focused on mean parameters and not on inter-individual variability. Therefore, it was only possible to calculate the standard error of the mean (SEM) for two parameters C_{max} and AUC_{last}.

The maximum concentration (C_{max}) and the time to reach it (T_{max}) were estimated from each tissue concentration versus the time profile.

For plasma or tissues, the total area under the time curve (AUC_{inf}) was determined using the linear trapezoidal rule with extrapolation to infinity. Extrapolation $AUC_{(Clast-inf)}$ was based on the following equation:

$$AUC_{(Clast-inf)} = \frac{C_{last}}{\lambda_z}$$

where C_{last} is the last observed concentration and λ_z the slope of the terminal phase.

Consequently, the AUC_{inf} was calculated by:

$$AUC_{inf} = AUC_{(0-Clast)} + AUC_{(Clast-inf)}$$

where $AUC_{(0-Clast)}$ is the AUC between 0 and C_{last}.

The terminal slope was estimated from the linear part of the terminal phase by at least three points, and was conserved if the coefficient of determination r^2 was > 0.95.

The half-life of compounds ($t_{1/2}\,\lambda_z$) was determined using λ_z by the following formula:

$$t_{1/2}\,\lambda_z = \frac{0.693}{\lambda_z}$$

Partial areas were also estimated by linear trapezoidal method between [0-1d], [1-5d], [5-17d], and [17d-65d] i.e. the treatment period, the first depuration period, the second period and the last period after the treatment respectively.

The mean residence time (MRT) was calculated using the linear trapezoidal rule between 0 and C_{last} or with extrapolation to infinity. Apparent total body clearance ($Cl_{tot/F}$) and apparent volume of distribution at steady state (Vss/F) were also determined by:

$$CL_{tot}/_F = \frac{Dose}{AUC_{inf}}$$

and

$$Vss/_F = MRT\ x\ CL_{ss}$$

For both the parent compound and its major metabolite, the time to reach the concentration at the LOQ was not measured. However, it was estimated by extrapolation using a simple exponential equation defined by the elimination rate and the apparent volume of distribution.

$$C = A \times e^{-\lambda_z \times t}$$

Where C is the tissue concentration, λ_z is the elimination rate and A is the fitted apparent constant.

2.6.2. Statistical analysis

Pharmacokinetic parameters (AUC_{last}, C_{max}) are expressed as arithmetic means, with associated standard error of the mean. The NCA sparse methodology calculates pharmacokinetics parameters based on the mean profile for all the individuals in the dataset. The NCA object calculates the standard error for the mean concentration curve's maximum value (Cmax), and for the area under the mean concentration curve from dose time through the final observed time. These parameters obtained in muscle and skin for VBPO and DLVBPO were compared by a *t* test. A level a significance of 5% was retained.

3. Results

3.1. Analytical method performance for VPBO analysis

Linear regression with 1/X weighting was selected as the regression model for the validation in muscle on three different days, yielding the best response function and the best accuracy profile among those tested. Quadratic regression with 1/X weighting was selected as the regression model for global validation in plasma, skin, and liver matrices. The global validation was performed on three days, with one day of validation for each matrix (Hubert et al., 2004; Hubert et al., 2007a; Hubert et al., 2007b). The corresponding results are presented in **Supplementary Table S1**.

Trueness was lower than 10% in recovery on the validation range from 0.5 to 50 µg.kg^{-1} (or µg.L^{-1} for plasma), except at 0.5 µg.kg^{-1} (or µg.L^{-1} for plasma) for the three combined matrices for which recovery was 112.3%. This value obtained for three matrices that were entirely different and at low concentrations, was however, considered satisfactory. For precision (repeatability and intermediate precision), relative standard deviations (RSDs) did not exceed 10% for muscle from 0.5 to 50 µg.kg^{-1}. At 0.5 µg.kg^{-1} (or µg.L^{-1}: plasma), RSDs did not exceed 15% for the combined plasma-skin-liver matrices.

The β-expectation tolerance interval limits (%) were within the acceptance limits (±50%) for both muscle and combined plasma-skin-liver matrices. This method is thus accurate from 0.5 to 50 µg.kg^{-1} (or µg.L^{-1} for plasma) for all matrices.

The limit of detection (LOD) was estimated at 0.15 µg.kg^{-1} (or µg.L^{-1} for plasma) for all matrices. The estimated lower and upper LOQs were 0.5 and 50 µg.kg^{-1} (or µg.L^{-1} for plasma). For muscle, the risk of error was below 0.1%. For the combined plasma-skin-liver matrices from 0.5 to 50 µg.kg^{-1} (or µg.L^{-1} for plasma), this risk was below 2%.

For muscle, the relative uncertainty was limited to 20%, and for the combined plasma-skin-liver matrices, it was limited to 17%, except at 0.5 µg.kg^{-1} (L^{-1} for plasma) (31%) (**Supplementary Table S2**).

The equations for the linearity of the results are provided in **Supplementary Table S3**. The coefficients of determination R^2 were above 0.99. The β-expectation tolerance interval limits were within the acceptance limits (±50%) for all matrices, regardless of the concentration of the validation standards, as shown in Supplementary **Figure S1.**

Supplementary Figure S1. Accuracy profiles concerning method validation for muscle (a) and plasma, skin, and liver (b).

Supplementary Table S1. Detailed results of method validation for all matrices (muscle, plasma, skin, and liver).

Supplementary Table S2. Estimated uncertainties of measurement at each concentration level of the validation samples.

Supplementary Table S3. Data regression analysis of the standard calibration curves.

3.2. Metabolites of VPBO

Metabolites were detected from the total ion current of chromatograms in muscle, plasma, skin, and liver by MetWorks software, and metabolites were then tentatively identified based on their accurate masses, mass errors, and retention times compared to VPBO retention times. As shown in **Table 1**, there were 15 metabolites of VPBO in total found in rainbow trout. The exact and measured masses matched with a mass error below 5 ppm, providing support for the proposed elemental compositions of metabolites. During the treatment period, the total amount of metabolites followed the order: liver > muscle ≅ plasma > skin. Otherwise, during the depuration period, the total amount of metabolites followed this order: muscle > skin ≅ liver > plasma. The intensities of signals for metabolites are shown in **Supplementary Figure S2**. The metabolites found in this animal experiment were quite similar to those found in a previous *in vitro* study (Dubreil et al., 2020b). However, we observed a few differences that are described below.

Phase I metabolites

297 The $[M]^+$ ions of metabolites M1 to M6 matched with dealkylation reactions regarding loss of masses of VPBO.
298 The same dealkylated metabolites were observed as those in the *in vitro* study except that the deethylation +
299 demethylation could not be observed *in vivo*. VPBO underwent successive deethylation for M1 to M5 (removal of
300 28.03130 Da) and demethylation for M6 (removal of 14.01565 Da). M1 (*m/z* 450.2903) to M5 (*m/z* 338.1651) had
301 retention times of 6.5, 6.0, 5.4, 5.0, and 4.7 min, respectively. Retention times decreased with the number of
302 deethylations, so the shortest retention time was assigned to quintuple N-deethylation (M5), consolidating the
303 proposed pathway of successive deethylations. Metabolite M6 had a retention time of 6.8 and showed $[M]^+$ ion at
304 m/z 464.3059.
305 Metabolites M8, M10, M11, M14, and M15 followed N-oxidation and also dehydrogenation for M14 and M15,
306 as cited in the previous *in vitro* study (Dubreil et al., 2020b). However, metabolites M7 (deethylation +
307 demethylation), M9 (deethylation + oxidation), M12 (oxidation + dehydrogenation), and M13 (deethylation +
308 oxidation + dehydrogenation) detected in the *in vitro* study were not observed *in vivo*. M8, M10, M11, M14, and
309 M15 eluted at 6.0, 5.5, 5.2, 5.1, and 4.8 min, respectively. Certain ions were observed at 16 Da higher compared
310 to the non-oxidized ion, for example M9 (deethylation + oxidation) compared to M1 (deethylation).
311 The double-bound reduction reaction was observed more strongly in treated rainbow trout than after *in vitro*
312 incubations for which the major metabolite identified was the deethyl-VPBO (M1) without the double-bound
313 reduction. Three proposed reactions were observed, (1) the double-bound reduction reaction which is also very
314 well described for triarylmethane dyes, (2) the double-bound reduction + deethylation reaction, and (3) the double-
315 bound reduction + double deethylation reaction. Only metabolite M16 corresponding to reaction (3) was observed
316 weakly during the previous *in vitro* incubation. Metabolite M17 could be proposed as the leuco form of VPBO at
317 *m/z* 480.3371 and eluted at 9.3 min. It was at least 10 times less intense than M16 in muscle and skin **(Table 2)**.
318 M18 was observed between 1.1 and 3.3 times more intense than M17 in muscle and skin, corresponding to double-
319 bound reduction + deethylation at *m/z* 424.2747 and retention time at 8.5 min. M16 was observed at least 10 times
320 more intense in muscle and skin compared to M17 and M18, which could explain why it was the only ion detected
321 *in vitro* that undergoes double-bound reduction. M16 was detected at *m/z* 452.3053 and retention time at 10.1 min.
322 The chromatograms of M16 and the parent VPBO are shown in **Figure 1**.
323 This *in vivo* metabolism study identified the most intense metabolite as M16 during the depuration period, as
324 shown in the mean peak areas of metabolites in **Supplementary Figure S2**. This deethyl-leuco metabolite was
325 found in the four matrices, and was also present in large amounts during the depuration period. Its identity was
326 confirmed by the CID fragment ions (*m/z*= 423.18, 379.39, 303.38, 252.37) and compared to the fragmentation of

the deethyl-VPBO carried out during a previous *in vitro* study. However, only one isomer could be retrieved *in vivo* compared to *in vitro* where two isomers where detected (Dubreil et al., 2020b). As a result, the deethyl-leuco VPBO (DLVPBO) was integrated in further data analysis to compare its pharmacokinetic parameters with those of VPBO.

Table 1. *In vivo* LC-Orbitrap-HRMS data for VPBO and its metabolites in rainbow trout. Metabolites M7, M9, M12, and M13 were not detected contrary to our previous *in vitro* study.

Table 2. Peak area ratios between main metabolites of VPBO detected in muscle, liver, plasma and skin during treatment and during depuration.

Figure 1. Chromatogram of VPBO and principal metabolite M16 deethyl-leuco-VPBO (DLVPBO) in muscle (at T12), liver (at T14), skin (at T5), and plasma (at T3).

Supplementary Figure S2. Mean peak area of VPBO metabolites detected in muscle, liver, plasma and skin during treatment and during depuration.

Phase II metabolite

A single ion M18 detected at m/z 670.3486 was found probably to be a glucuronide metabolite with supplementary oxidation, corresponding to the difference in mass of *m/z* 192.0270 with VPBO. This ion was only detected in liver during the treatment and depuration periods. The error on the measured mass was 1.49 ppm, which is low. Moreover, the retention time was 5.3 min, indicating that this ion eluted earlier than VPBO. The retention time of M18 supported the assumption of its identification as a glucuronide. In fact, glucuronide metabolites are classified as phase II metabolites and as a rule, offer weaker retention because of the high polarity of the glucuronide part.

3.3. Comparative pharmacokinetic analysis of VPBO and major metabolite DLVPBO in rainbow trout

3.3.1 Uptake and depuration of VPBO in different tissues

Water bath exposure of rainbow trout in a tank containing 0.1 $mg.L^{-1}$ of VPBO for one day did not lead to deaths. VPBO was well tolerated by the exposed rainbow trout. At each time point, matrices (muscle, plasma, skin, and

liver) were sampled carefully to carry out the analysis of residues of VPBO in each matrix by the validated LC-HRMS method. The mean concentrations of VPBO (±SD, standard deviation) in muscle, plasma, skin, and liver are shown in **Table 3**.

During the uptake period, the mean VPBO concentrations in muscle and skin increased until the last sampling time point at 24h (T4) and were measured at 99.9 $\mu g.kg^{-1}$ ±54.4 for muscle, and 263 $\mu g.kg^{-1}$ ±78.2 for skin. Unlike this increase, the highest concentrations for plasma and liver occurred at the first date of sampling at 2 hours (T1) after the beginning of treatment. The concentrations were 567 $\mu g.L^{-1}$ ±300 for plasma and 1,846 $\mu g.kg^{-1}$ ±517 for liver. These levels decreased subsequently during the uptake period. At the end of the uptake period after 24 h, the highest concentration levels in matrices followed this order: liver > skin > muscle > plasma. The plasma concentrations decreased rapidly during this period from 567 $\mu g.L^{-1}$ ±300 at T1 to 9.27 $\mu g.L^{-1}$ ±7.35 at T4 **(Supplementary Figure S3)**.

After placing the rainbow trout in a clean water bath for depuration, the concentrations in the tissues and plasma decreased gradually over the 64 days of depuration. At the end of this period, concentrations were still above the LOQ for muscle, skin and liver. VPBO was barely detectable in plasma, with concentrations below the LOQ at 5 days (T7) after withdrawal of treatment. The levels reached in muscle and skin were comparable after 33 days and were measured at 2.26 $\mu g.kg^{-1}$ ±0.48 for muscle and 2.85 $\mu g.kg^{-1}$ ±1.99 for skin at the end of the depuration period.

Table 3. Concentrations of VPBO in muscle, plasma, skin, and liver of rainbow trout after exposure to VPBO (n=6 trout) at a dose of 40 $mg.kg^{-1}$ b.w.

Supplementary Figure S3. Mean concentration profile of VBPO in rainbow trout tissues and plasma after water bath for 24 h with VPBO at a dose of 40 $mg.kg^{-1}$ b.w.

3.3.2 Pharmacokinetic analysis of VPBO and DLVPBO

Pharmacokinetic parameters were determined using sparse sampling non-compartmental analysis and are presented in **Table 4** for VPBO in plasma and tissues and for DLVPBO in only muscle and skin, because it is edible tissue, and based on the calibration model of VPBO since no standard product is available for DLVPBO.

Parent VPBO

The maximum plasma concentration C_{max} (567 ± 301 $\mu g.L^{-1}$) after water bath treatment was reached at time T_{max} of 0.083 d (2 h) for VPBO, demonstrating rapid absorption. The apparent total body clearance (Cl_{tot}/F) was 0.34

$L.kg^{-1}.d^{-1}$ for plasma. The apparent volume of distribution at steady state (Vss/F) was 0.095 $L.kg^{-1}$. The elimination half-life ($t_{1/2}\,\lambda_z$) in plasma was short, (0.73 day) compared to other tissues. The area under the curve, AUC_{inf}, was calculated as 116 $\mu g.d.L^{-1}$. The initial distribution of VPBO in tissues showed the highest concentration C_{max} in liver at 1,847 $\mu g.kg^{-1}$ ± 211, at 99.9 $\mu g.kg^{-1}$ ± 22.2 in muscle, and at 264 $\mu g.kg^{-1}$ ± 35.9 in skin, occurring at T_{max} of 0.083 days (2 hours) for liver, and at 1 d for muscle and 2 d for skin. AUC_{inf} in skin estimated at 2,781 $\mu g.d.kg^{-1}$ was 2 and 2.75 times higher than in liver and muscle, respectively. The mean residence time (MRT_{inf}) was longer in skin and muscle , with values of 12.7 and 20.7 days respectively, compared to liver (5 days). The terminal elimination phase was the longest in muscle with a $t_{1/2}\,\lambda_z$ estimated at 17.1 days.

Main metabolite: DLVPBO

For the main metabolite identified, DLVPBO, the parameters were assessed only in muscle and skin (**Table 4**). The different pharmacokinetic profiles between the parent VPBO and the major metabolite DLVPBO are plotted in **Figure 2**. The C_{max} values were lower for DLVPBO estimated at 31 $\mu g.kg^{-1}$ ± 3.8 in muscle and 70.6 $\mu g.kg^{-1}$ ± 9.0 in skin. A lower elimination rate of DLVPBO, and consequently a terminal elimination phase, was observed in muscle (22.5 days) compared to the elimination rate of VPBO (18.1 days). The mean residence time (MRT_{inf}) was estimated to be 43.1 days in muscle and 29.9 days in skin for DLVPBO, versus 20.7 days and 12.7 days for VPBO respectively. The computations of partial areas of VPBO and DLVPBO for different sampling times in muscle and skin showed systematically higher concentrations of parent compound compared to DLVBPO, in all period. (**Figure 3**).

Table 4. Pharmacokinetic parameters of VPBO determined by sparse sampling non-compartmental analysis in rainbow trout tissue and plasma, and of metabolite DLVPBO in muscle and skin after a water bath of rainbow trout in a bath containing 40 $mg.kg^{-1}$ b.w. of VBPO for 24 h.

Figure 2. Concentration profile of VPBO and DLVPBO in rainbow trout muscle (a) and skin (b) after water bath with VBPO at a dose of 40 $mg.kg^{-1}$ b.w.

Figure 3. Partial area ($\mu g.day.kg^{-1}$) of VPBO and DLVPBO for different time points in rainbow trout muscle (a) and skin (b).

4. Discussion

This study assessed for the first time the metabolism, pharmacokinetics and tissue residues in rainbow trout exposed to VPBO dye in a water bath. During a preliminary test (data not shown), high toxicity of VPBO was observed for a dose at 0.8 $mg.L^{-1}$. Different concentrations of malachite green MG in bath treatment for aquaculture are depicted in the literature. The concern is always about the potential for human toxicity in the presence of malachite and leucomalachite green in fish tissues. Alderman and Clifton-Hadley (1993) exposed rainbow trout to 1.6 $mg.L^{-1}$ of MG for 40 min, at two different temperatures. Máchová et al (1996) applied treatment of rainbow trout at 0.2 $mg.L^{-1}$ of MG for 6 days in a water bath. Bajc et al (2011) chose to apply different doses ranging from 1 $mg.L^{-1}$ to 1.5 $mg.L^{-1}$ of waterborne MG for different exposure times (1h or 3h). These studies could only provide a guide for waterborne treatment of rainbow trout by triarylmethane-like dyes because no data could be retrieved for the administration of VPBO in aquaculture. However, in our previous metabolomics study, a dose of 0.05 $mg.L^{-1}$ for rainbow trout exposed to VPBO for two days was applied following the experimental design by Dubreil et al. (2019b). The number of metabolites found in the metabolomics study was quite low (5 metabolites) compared to all those found in the *in vitro* study (15 metabolites). So a higher concentration was tested at 0.1 mg/L demonstrating notoxicity for the fish (Dubreil et al., 2019a; Dubreil et al., 2020b). The final dose of 0.1 $mg.L^{-1}$ of VPBO diluted in a water bath for one day was selected.

The first step in this study was to examine the metabolites obtained and potentially the main relevant metabolite, that could be even more persistent than the parent compound VPBO. The determination of a persistent metabolite as a marker residue is important to track administration of a treatment over time after fish exposure to the prohibited substance. In addition, this marker residue can be more toxic than the parent compound. Takal and Özer (2007) found that the generation of triarylmethane metabolites did not alter the toxic load on exposed organisms because metabolites were at least as toxic as the parent compounds. Our *in vitro* metabolite investigation demonstrated that VPBO is biotransformed into 15 metabolites in the different biological tissues of rainbow trout, with in particular a greater amount of metabolites detected in liver (Dubreil et al., 2020b). During the treatment period in this study, the total amount of metabolites (expressed in peak area) followed this order: liver > skin ≅ plasma > muscle, whereas during the depuration period, the total amount of metabolites followed this order: liver > skin ≅ muscle > plasma. This estimated metabolic rate was in line with the rapid depuration by the liver found for other triarylmethane dyes with a similar structure (Plakas et al., 1996; Decroos et al., 2009). Furthermore, high levels of total MG residues in the liver of channel catfish (*Ictalurus punctatus*) for two weeks after waterborne exposure to a C^{14}-MG solution were reported by Plakas et al. (1996). In addition, the liver, along with the gills, is an organ of major importance in the ecotoxicology of fish due to its high metabolic capacities and its crucial role in

451 detoxification (Gomez et al., 2010). In this study, VPBO was metabolized particularlyinto M16, M15 and M17 in
452 muscle, plasma and skin during the depuration period, as well as into M16 and M17 in the liver. These metabolites
453 correspond to m/z 452,3060 (M16, proposed as N-deethyl-leuco VPBO or DLVPBO), m/z 408.2069 (M15,
454 proposed as N-oxidated dehydrogenated triple N-deethyl VPBO), and m/z 480,3373 (M17, proposed as leuco-
455 VPBO). The metabolites found (the main metabolite and the others identified), suggest that dealkylation
456 (deethylation) and double-bound reduction are major metabolic pathways. The M16 was also found in our previous
457 metabolomics study (Dubreil et al., 2019b), ranking first in muscle, and third in the liver. In the same metabolomics
458 study, the M17 was also detected, ranking first in the liver, but not detected in muscle, whereas it was detected in
459 high amounts in the present study in muscle. Similar pathways of dealkylation and oxidation for MG were
460 described by Doerge et al. (1998), showing that levels of leucoMG in edible tissues of fish exceeded those of MG,
461 and consequently confirmed that leuco-MG was a relevant residue marker for regulatory determination of MG
462 misuse. In this study on VPBO, a substance derived from a triarylmethane structure similar to MG, we found that
463 the metabolite leading to the highest signal intensity in all biological matrices was M16, proposed as DLVPBO.
464 The assessment of pharmacokinetic parameters was first carried out for the parent compound. During the uptake
465 period, the concentration of VPBO in plasma and liver increased rapidly, and concentrations were the highest at
466 the beginning of the treatment, suggesting efficient uptake by the gills, and to a lesser degree by skin then muscle.
467 The role of the gills in the uptake of MG, a similar triarylmethane dye, was described for the first time by Poe and
468 Wilson (1983). The high concentration of VPBO in liver was directly associated to the role of liver, where hepatic
469 biotransformation directly relates to bioaccumulation of lipophilic contaminants in fresh water fish (Schultz et al.,
470 1999). Moreover, an increase in concentrations was observed at the end of the uptake period for muscle and skin,
471 probably due to reabsorption of VPBO via excrements eliminated in the closed water bath. To the best of our
472 knowledge, no data are available on the level of VPBO after treatment in fish for comparison. During our study, a
473 rapid decline of VPBO was observed in plasma. The elimination half-life was calculated as 0.73 days (around 18
474 h) in plasma. For MG, Alderman and Clifton-Hadley (1993) determined $t_{1/2}\,\lambda_z$ of trout plasma to be 0.62 days at
475 8°C, and 14.5 days at 16°C, so a longer elimination rate with the increasing of temperature. In the present study,
476 rainbow trout were kept at 13°C in a water bath, and temperature has been described elsewhere as a key factor for
477 the elimination of MG as well as other environmental factors (Lanzing, 1965). VPBO tends to be eliminated faster
478 than MG around the same temperature, presumably because it is bio-transformed into a broader panel of
479 metabolites. In tissues, the decrease in VPBO concentrations was slower than in plasma. Our results show that the
480 mean residence time of VPBO in muscle and skin, was higher than in liver and plasma.

For the major metabolite identified, DLVPBO, the amount of metabolite (in peak area) was converted in concentration considering the same analytical response than the parent VPBO; the concentrations were assessed only for muscle and skin in order to estimate pharmacokinetic parameters for DLVPBO in the edible matrix that need a definition of residue marker. The estimated C_{max} values in muscle and skin were three and eight times lower than those of the parent compound, respectively but mean residence times were higher for the metabolite. In fact, LVPBO tend to decrease more slowly than its parent molecule taking into account the biologic variability. The elimination half-life in muscle and skin was slightly higher compared to VPBO, which confirmed the same fate of DLVPBO as the main metabolite of MG (LMG). In fact, Plakas et al (1996) demonstrated that MG and LMG half-lives in catfish muscle were 2.8 and 10 days, respectively. MG and LMG were also more persistent in muscle than in plasma, with a major role of metabolism in the clearance of the parent compound. The difference in elimination rates between the parent compound MG and its metabolite residue marker LMG seems more pronounced than for VPBO and DLVPBO. This could be due to lipid content because in the Plakas et al (1996) study, the model was evaluated for catfish, which is a fattier fish species than rainbow trout, and LMG accumulates in fat. In addition, MG is less lipophilic than VPBO (log P (MG)= 0.62 and estimated log P (VPBO)= 4.06). Fat content has actually been proven to act on metabolite levels. In a study on carp and trout, Jiang et al (2009) found that there was a difference between three common freshwater fish, *Parabramispekinensis* (plant-eating fish), *Carassiusauratus* (omnivorous fish) and *Ophiocephalusargus* (carnivorous fish), with LMG levels significantly correlated with lipid content in fish tissue. In our study, the rainbow trout were not very fatty, weighing a mean of 117 g at the start and 232 g at the end of the experiment. As a result, differences could be found for the depuration rates of VPBO and DLVPBO in other fatty fish.

The time needed for the metabolite DLVPBO concentration to decrease below to the LOQ (LOQ = 0.5 $\mu g.kg^{-1}$) was 149 days in edible muscle tissue, whereas it appears to be shorter for VPBO (110 days). It may be beneficial to investigate this tendency in other fish species. Our results, showing longer persistence of the DLVPBO metabolite in muscle and especially in skin, compared to parent VPBO, are of particular interest. The concentrations found in the skin highlighted that monitoring of VPBO for food safety or environmental contamination should not dissociate the muscle from the skin. This study demonstrated that the bioaccumulation of VPBO and some metabolite residues in edible fish tissues is an important aspect for consumer's health regulatory agencies should be aware of. However, these results should be interpreted with caution to take into account the *in vivo* variability. It would be necessary to produce a toxicological assessment of DLVPBO in order

to propose definitely the sum of VPBO and DLVPBO as the relevant residue marker of an illegal treatment by VPBO in farmed rainbow trout.

5. Conclusion

The results of the current study demonstrate that VPBO is rapidly absorbed and well distributed in rainbow trout muscle, skin, and liver, after water bath administration for one day. VPBO is then rapidly converted into 15 metabolites, with one metabolite found to be more intense and persistent, proposed as deethyl-leuco-VPBO (DLVPBO). These results highlight the key role played by the liver in the metabolism of VPBO. A depuration period of 60 days enabled us to compare the pharmacokinetic profiles of VPBO and DLVPBO. The metabolic profiles showed that the parent drug VPBO occurs at higher concentrations in muscle and skin at the start of the uptake period, but its concentrations fall below those of DLVPBO after 17 days. At 60 days of depuration, the concentrations of VPBO in muscle and skin (mean of 2.5 $\mu g.kg^{-1}$) are still slightly above the limit of quantification of 0.5 $\mu g.kg^{-1}$, whereas concentrations of the DLVPBO metabolite were found to be a mean of 8.8 $\mu g.kg^{-1}$ in the same tissues. For these reasons, VPBO and its major metabolite DLVPBO, an appropriate residue marker, should both be monitored without dissociating adhering skin, for effective residue control.

Declaration of Competing interest

The authors declare that they have no known competing financial interests or personal relationships that could have appeared to influence the work reported in this paper.

Acknowledgement

The authors thank the European Commission Directorate-General for Health and Food Safety (European contribution to the European Union Reference Laboratory SI2.726842 & SI2.777451), which enabled this work to be carried out.

References

Alderman, D.J., 1982. In vitro testing of fisheries chemotherapeutants. Journal of Fish Diseases 5, 113-123.

Alderman, D.J., 1985. Malachite green: a review. Journal of Fish Diseases 8, 289-298.

Alderman, D.J., Clifton-Hadley, R.S., 1993. Malachite green: a pharmacokinetic study in rainbow trout, Oncorhynchus mykiss (Walbaum). Journal of Fish Diseases 16, 297-311.

Bajc, Z., Jenčič, V., Šinigoj Gačnik, K., 2011. Elimination of malachite green residues from meat of rainbow trout and carp after water-born exposure. Aquaculture 321, 13-16.
Bergwerff, A.A., Kuiper, R.V., Scherpenisse, P., 2004. Persistence of residues of malachite green in juvenile eels (Anguilla anguilla). Aquaculture 233, 55-63.
Culp, S.J., Blankenship, L.R., Kusewitt, D.F., Doerge, D.R., Mulligan, L.T., Beland, F.A., 1999. Toxicity and metabolism of malachite green and leucomalachite green during short-term feeding to Fischer 344 rats and B6C3F1 mice. Chemico-Biological Interactions 122, 153-170.
CVMP, 1998. Establishment of maximum residue limits for Salmonidae and other fin fish.
Decroos, C., Li, Y., Bertho, G., Frapart, Y., Mansuy, D., Boucher, J.L., 2009. Oxidative and reductive metabolism of tris(p-carboxyltetrathiaaryl)methyl radicals by liver microsomes. Chemical Research in Toxicology 22, 1342-1350.
Dervilly-Pinel, G., Chereau, S., Cesbron, N., Monteau, F., Le Bizec, B., 2015. LC-HRMS based metabolomics screening model to detect various β-agonists treatments in bovines. Metabolomics 11, 403-411.
Doerge, D.R., Churchwell, M.I., Gehring, T.A., Pu, Y.M., Plakas, S.M., 1998. Analysis of malachite green and metabolites in fish using liquid chromatography atmospheric pressure chemical ionization mass spectrometry. Rapid Communications in Mass Spectrometry 12, 1625-1634.
Dubreil, E., Mompelat, S., Kromer, V., Guitton, Y., Danion, M., Morin, T., Hurtaud-Pessel, D., Verdon, E., 2020a. Corrigendum to "Dye residues in aquaculture products: Targeted and metabolomics mass spectrometric approaches to track their abuse [Food Chem. 294 (2019) 355–367]. Food Chemistry 306, 125539.
Dubreil, E., Mompelat, S., Kromer, V., Guitton, Y., Danion, M., Morin, T., Hurtaud-Pessel, D., Verdon, E., 2019. Dye residues in aquaculture products: Targeted and metabolomics mass spectrometric approaches to track their abuse. Food Chemistry 294, 355-367.
Dubreil, E., Sczubelek, L., Burkina, V., Zlabek, V., Sakalli, S., Zamaratskaia, G., Hurtaud-Pessel, D., Verdon, E., 2020b. In vitro investigations of the metabolism of Victoria pure blue BO dye to identify main metabolites for food control in fish. Chemosphere 238.
EFSA, Penninks, A., Baert, K., Levorato, S., Binaglia, M., 2017. Dyes in aquaculture and reference points for action. EFSA Journal 15, e04920.
Gallart-Ayala, H., Chéreau, S., Dervilly-Pinel, G., Bizec, B.L., 2015. Potential of mass spectrometry metabolomics for chemical food safety. Bioanalysis 7, 133-146.
Gessner, T., Mayer, U., 2000. Triarylmethane and Diarylmethane Dyes. Ullmann's Encyclopedia of Industrial Chemistry.
Gomez, C.F., Constantine, L., Huggett, D.B., 2010. The influence of gill and liver metabolism on the predicted bioconcentration of three pharmaceuticals in fish. Chemosphere 81, 1189-1195.
Hubert, P., Nguyen-Huu, J.J., Boulanger, B., Chapuzet, E., Chiap, P., Cohen, N., Compagnon, P.A., Dewé, W., Feinberg, M., Lallier, M., Laurentie, M., Mercier, N., Muzard, G., Nivet, C., Valat, L., 2004. Harmonization of strategies for the validation of quantitative analytical procedures: A SFSTP proposal - Part I. Journal of Pharmaceutical and Biomedical Analysis 36, 579-586.
Hubert, P., Nguyen-Huu, J.J., Boulanger, B., Chapuzet, E., Chiap, P., Cohen, N., Compagnon, P.A., Dewé, W., Feinberg, M., Lallier, M., Laurentie, M., Mercier, N., Muzard, G., Nivet, C., Valat, L., Rozet, E., 2007a. Harmonization of strategies for the validation of quantitative analytical procedures. A SFSTP proposal - Part II. Journal of Pharmaceutical and Biomedical Analysis 45, 70-81.
Hubert, P., Nguyen-Huu, J.J., Boulanger, B., Chapuzet, E., Cohen, N., Compagnon, P.A., Dewé, W., Feinberg, M., Laurentie, M., Mercier, N., Muzard, G., Valat, L., Rozet, E., 2007b. Harmonization of strategies for the validation of quantitative analytical procedures. A SFSTP proposal-Part III. Journal of Pharmaceutical and Biomedical Analysis 45, 82-96.
Jiang, Y., Xie, P., Liang, G., 2009. Distribution and depuration of the potentially carcinogenic malachite green in tissues of three freshwater farmed Chinese fish with different food habits. Aquaculture 288, 1-6.
Kwan, P.P., Banerjee, S., Shariff, M., Yusoff, F.M., 2020. Persistence of malachite green and leucomalachite green in red tilapia (Oreochromis hybrid) exposed to different treatment regimens. Food Control 108.
Lanzing, W.J.R., 1965. Observations on malachite green in relation to its application to fish diseases. Hydrobiologia 25, 426-441.
Lewis, L.M., Indig, G.L., 2002. Effect of dye aggregation on triarylmethane-mediated photoinduced damage of hexokinase and DNA. Journal of Photochemistry and Photobiology B: Biology 67, 139-148.
Lewis, L.M., Indig, G.L., 2001. Photonuclease activity of mitochondrial triarylmethane photosensitizers. Pharmaceutical and Pharmacological Letters 11, 22-25.
Máchová, J., Svobodová, Z., Svobodník, J., Piačka, V., Vykusová, B., Kocová, A., 1996. Persistence of malachite green in tissues of rainbow trout after a long-term therapeutic bath. Acta Veterinaria Brno 65, 151-159.

Ngan, D.K., Ye, L., Wu, L., Xia, M., Rossoshek, A., Simeonov, A., Huang, R., 2019. Bioactivity Signatures of Drugs vs. Environmental Chemicals Revealed by Tox21 High-Throughput Screening Assays. Frontiers in Big Data 2.
Okocha, R.C., Olatoye, I.O., Adedeji, O.B., 2018. Food safety impacts of antimicrobial use and their residues in aquaculture. Public Health Reviews 39.
Plakas, S.M., El Said, K.R., Stehly, G.R., Gingerich, W.H., Allen, J.L., 1996. Uptake, tissue distribution, and metabolism of malachite green in the channel catfish [Ictalurus punctatus]. Canadian Journal of Fisheries and Aquatic Sciences 53, 1427-1433.
Poe, W.E., Wilson, R.P., 1983. Absorption Of malachite green by channel catfish. Progressive Fish-Culturist 45, 228-229.
RASFF-portal, European Commission. https://webgate.ec.europa.eu/rasff-window/portal/.
Roberts, R.J., Ellis, A.E., 2012. The Anatomy and Physiology of Teleosts. Fish Pathology: Fourth Edition, pp. 17-61.
Schnick, R.A., 1988. The impetus to register new therapeutants for aquaculture. Progressive Fish-Culturist 50, 190-196.
Schultz, I.R., Hayton, W.L., 1999. Interspecies scaling of the bioaccumulation of lipophilic xenobiotics in fish: An example using trifluralin. Environmental Toxicology and Chemistry 18, 1440-1449.
Srivastava, S., Sinha, R., Roy, D., 2004. Toxicological effects of malachite green. Aquatic Toxicology 66, 319-329.
Sudova, E., Machova, J., Svobodova, Z., Vesely, T., 2007. Negative effects of malachite green and possibilities of its replacement in the treatment of fish eggs and fish: A review. Veterinarni Medicina 52, 527-539.
Tacal, O., Özer, I., 2007. An assessment of the role of intracellular reductive capacity in the biological clearance of triarylmethane dyes. Journal of Hazardous Materials 149, 518-522.
Verdon, E., Bessiral, M., Chotard, M.P., Couëdor, P., Fourmond, M.P., Fuselier, R., Gaugain, M., Gautier, S., Hurtaud-Pessel, D., Laurentie, M., Pirotais, Y., Roudaut, B., Sanders, P., 2015. The monitoring of triphenylmethane dyes in aquaculture products through the European Union network of official control laboratories. Journal of AOAC International 98, 649-657.

Figure 1. Chromatogram of VPBO and principal metabolite M16 deethyl-leuco-VPBO (DLVPBO) in muscle (at T12), liver (at T14), skin (at T5), and plasma (at T3).

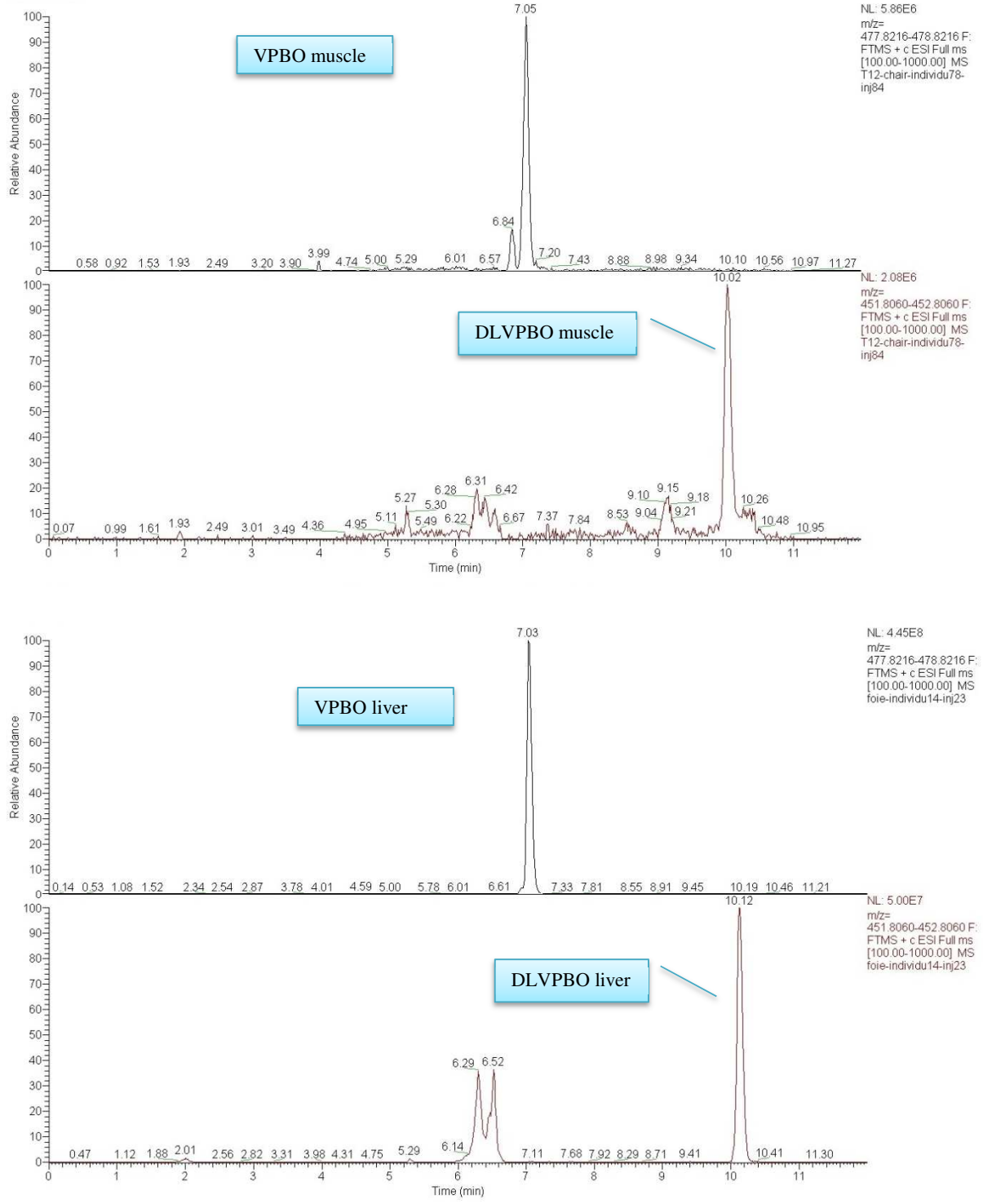

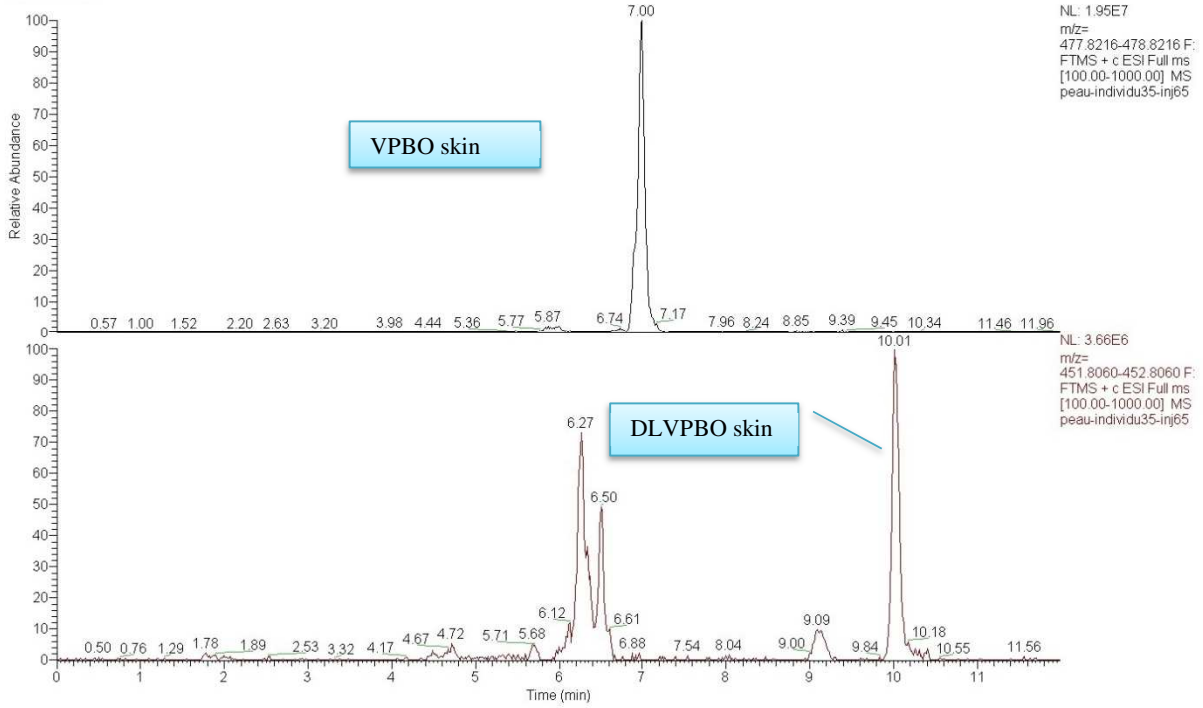
VPBO skin
NL: 1.95E7
m/z=
477.8216-478.8216 F:
FTMS + c ESI Full ms
[100.00-1000.00] MS
peau-individu35-inj65
DLVPBO skin
NL: 3.66E6
m/z=
451.8060-452.8060 F:
FTMS + c ESI Full ms
[100.00-1000.00] MS
peau-individu35-inj65
Relative Abundance
Time (min)

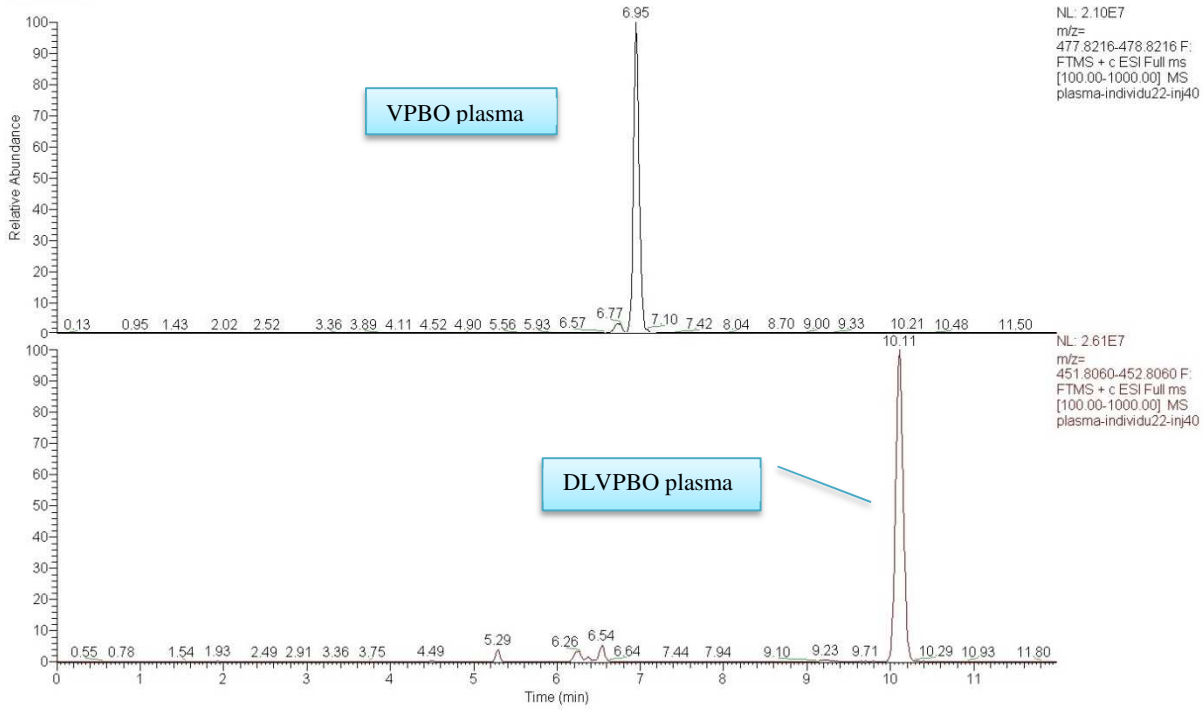
VPBO plasma
NL: 2.10E7
m/z=
477.8216-478.8216 F:
FTMS + c ESI Full ms
[100.00-1000.00] MS
plasma-individu22-inj40
DLVPBO plasma
NL: 2.61E7
m/z=
451.8060-452.8060 F:
FTMS + c ESI Full ms
[100.00-1000.00] MS
plasma-individu22-inj40
Relative Abundance
Time (min)

Figure 2. Concentration profile of VPBO and DLVPBO in rainbow trout muscle (a) and skin (b) after water bath with VBPO at a dose of 40 mg.kg^{-1} b.w.

(a)

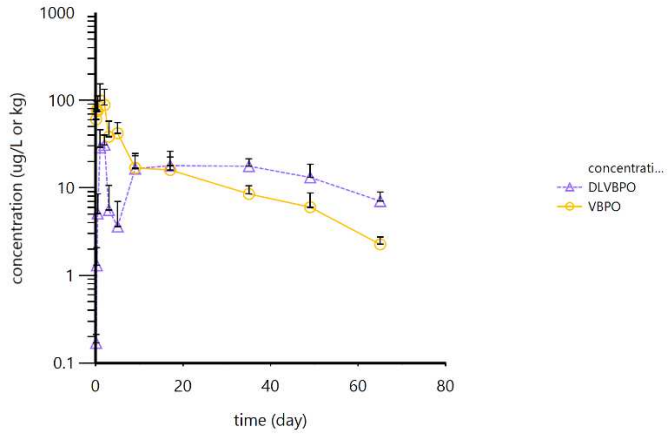

(b)

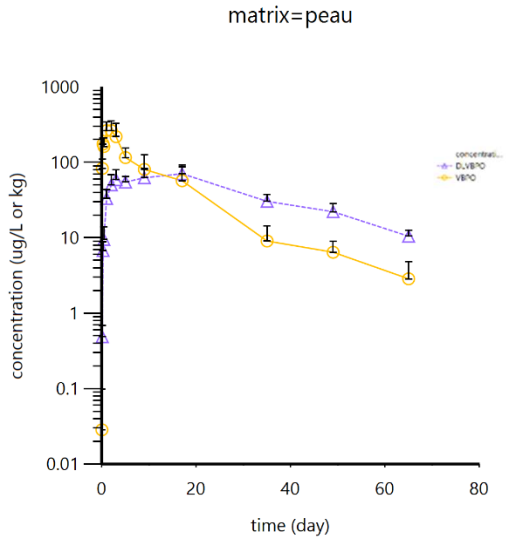

Figure 3. Partial area (µg.day^{-1}.kg^{-1}) of VPBO and DLVPBO for different time points in rainbow trout muscle (a) and skin (b).

(a)

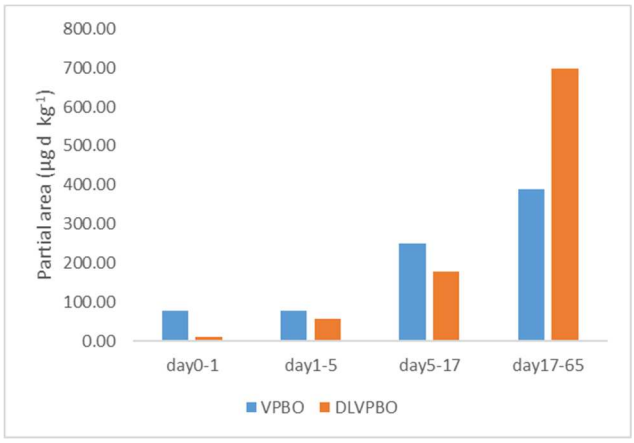

(b)

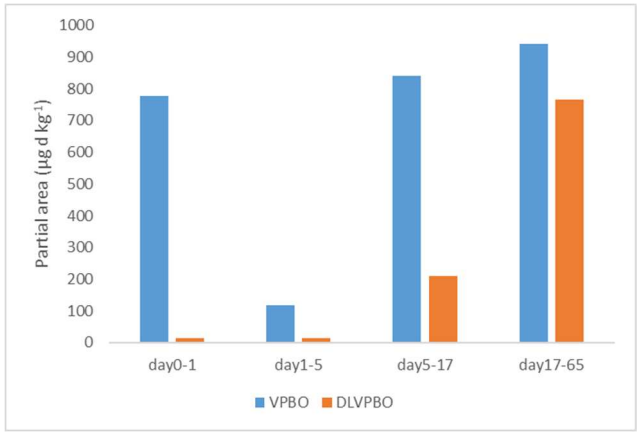

Table 1. *In vivo* LC-Orbitrap-HRMS data for VPBO and its metabolites in rainbow trout. Metabolites M7, M9, M12, and M13 were not detected contrary to our previous *in vitro* study (ND: non detected).

Compound ID	Reaction proposed	Δm/z	Molecular formula	Calculated mass	Measured mass	Error (ppm)	RT (min)
M0 (VPBO)	/	/	$C_{33}H_{40}N_3$	478,3216	478,3205	2,3	7,1
M1	N-deethylation	-28,0313	$C_{31}H_{36}N_3$	450,2903	450,2895	1,77	6,5
M2	double N-deethylation	-56,0626	$C_{29}H_{32}N_3$	422,259	422,2583	1,65	6,0
M3	triple N-deethylation	-84,0939	$C_{27}H_{28}N_3$	394,2277	394,227	1,77	5,4
M4	quadruple N-deethylation	-112,1252	$C_{25}H_{24}N_3$	366,1964	366,1958	1,64	5,0
M5	quintuple N-deethylation	-140,1565	$C_{23}H_{20}N_3$	338,1651	338,1646	1,48	4,7
M6	N-demethylation	-14,0157	$C_{32}H_{38}N_3$	464,3059	464,305	1,94	6,8
M7	N-deethylation + N-demethylation	-42.0470	$C_{30}H_{34}N_3$	436.2746	ND	ND	ND
M8	N-oxidation	15,9949	$C_{33}H_{40}N_3O$	494,3165	494,3158	1,41	6,0
M9	N-deethylation + N-oxidation	-12.0364	$C_{31}H_{36}N_3O$	466.2852	ND	ND	ND
M10	N-oxidation + double N-deethylation	-40,0677	$C_{29}H_{32}N_3O$	438,2539	438,2538	0,23	5,5
M11	N-oxidation + triple N-deethylation	-68,0990	$C_{27}H_{28}N_3O$	410,2226	410,2221	1,21	5,2
M12	N-oxidation + deshydrogenation	13.9792	$C_{33}H_{38}N_3O$	492.3008	ND	ND	ND
M13	N-deethylation + N-oxidation + deshydrogenation	-14.0521	$C_{31}H_{34}N_3O$	464.2695	ND	ND	ND
M14	N-oxidation + deshydrogenation + double N-deethylation	-42,0833	$C_{29}H_{30}N_3O$	436,2382	436,2377	0,06	5,1
M15	N-oxidation + deshydrogenation + triple N-deethylation	-70,1146	$C_{27}H_{26}N_3O$	408,2069	408,2063	1,47	4,8
M16	double-bound reduction + N-deethylation	-26,0157	$C_{31}H_{38}N_3$	452,3060	452,3053	1,54	10,1
M17	double-bound reduction	2,0156	$C_{33}H_{42}N_3$	480,3373	480,3371	0,42	9,3
M18	double-bound reduction + double N-deethylation	-54,0470	$C_{29}H_{34}N_3$	424,2747	424,2739	1,89	8,5
M19	glucuronidation + N-oxidation	192,0270	$C_{39}H_{48}N_3O_7$	670,3486	670,3476	1,49	5,3

Table 2. Peak area ratios between main metabolites of VPBO detected in muscle, liver, plasma and skin during treatment and during depuration

Peak area ratios between main metabolites of VPBO	**Treatment**				**Depuration**			
	muscle	liver	plasma	skin	muscle	liver	plasma	skin
M16/M1	11	1	24	4	63	6	273	21
M16/M17	57	356	17	33	16	25	9	29
M16/M18	23	12	105	10	15	5	28	11
M18/M17	2.5	30.2	0.2	3.3	1.1	5.2	0.2	2.6

Table 3. Concentrations of VPBO in muscle, plasma, skin, and liver of rainbow trout after exposure to VPBO (n=6 trout) at a dose of 40 $mg.kg^{-1}$ b.w.

Date of treatment		Muscle $\mu g.kg^{-1}$ (**mean**±SD)	Plasma $\mu g.L^{-1}$ (**mean**±SD)	Skin $\mu g.kg^{-1}$ (**mean**±SD)	Liver $\mu g.kg^{-1}$ (**mean**±SD)
Uptake period (in days)					
T0	0	0	0	0	0
T1	0.083 d (2h)	**60.50±**13.34	**566.64±**300.54	**83.01±**27.26	**1846.08±**517.26
T2	0.208 d (6h)	**77.86±**20.68	**138.03±**101.29	**174.98±**35.92	**1468.48±**687.17
T3	0.417 d (10 h)	**75.30±**39.94	**32.15±**21.38	**162.02±**49.08	**825.21±**674.09
T4	1 d (24h)	**99.91±**54.43	**9.27±**7.35	**263.54±**78.17	**300.32±**131.21
Depuration period (in days)					
T5	2 d	**88.51±**44.72	**1.83±**2.35	**263.95±**88.03	**67.29±**30.78
T6	3 d	**38.39±**19.49	**0.51±**0.37	**219.05±**110.80	**56.95±**44.93
T7	5 d	**42.08±**13.82	<LOQ	**115.68±**39.65	**17.77±**8.41
T8	9 d	**16.89±**7.79	<LOD	**80.54±**45.34	**8.67±**3.96
T9	17 d	**16.01±**6.56	<LOQ	**56.94±**29.82	**3.24±**1.58
T10	34 d	**8.52±**2.03	<LOQ	**9.05±**5.22	**2.17±**1.00
T11	49 d	**6.02±**2.73	<LOD	**6.42±**2.54	**2.89±**3.30
T12	65 d	**2.26±**0.48	<LOD	**2.85±**1.99	**0.60±**0.39

Table 4. Pharmacokinetic parameters of VPBO determined by sparse sampling non-compartmental analysis in rainbow trout tissue and plasma, and of metabolite DLVPBO in muscle and skin after a water bath of rainbow trout in a bath containing 40 $mg.kg^{-1}$ b.w. of VBPO for 24 h.

	Parent VPBO				**DLVPBO**	
	liver	**plasma**	**muscle**	**skin**	**muscle**	**skin**
λ_z (d^{-1})	0.0443	0.9451	0.0406	0.0634	0.0310	0.0384
$T_{1/2}$ λ_z (d)	15.6	0.73	17.1	10.9	22.5	18.1
AUC_{last} ($\mu g.d.L^{-1}$ or kg^{-1}) ±SEM	1406 ± 130	116 ± 17	955 ± 57[(a)]	2736 ±219[(a)]	945 ± 64[(a)]	2528 ± 143[(a)]
AUC_{inf} ($\mu g.d.L^{-1}$ or kg^{-1})	1420	116	1010	2781	1175	2780
AUC_{extrap} (%)	0.96	0.17	5.52	1.62	19.53	9.72
Cl_{tot}/F ($L.kg^{-1}.d^{-1}$)	0.0281	0.34	0.0396	0.0144	0.0334	0.0143
MRT_{inf} (d)	5.03	0.28	20.7	12.7	43.1	29.9
Vss/F ($L.kg^{-1}$)	0.142	0.095	0.819	0.183	1.46	0.430
T_{max} (d)	0.083	0.083	1.00	2.00	2.00	17.0
C_{max} ($\mu g.L^{-1}$ or kg^{-1}) ±SEM	1847 ± 211	567 ± 123	99.9 ± 22.2[(b)]	264 ± 35.9[(b)]	31.0 ± 3.8[(b)]	70.6±9.0[(b)]

λ_z first order rate constant associated with the terminal portion of the curve; $T_{1/2}$ λ_z: terminal half-life; AUC_{last}: area under the curve (AUC) from time of dosing (0) to the time of the last quantifiable concentration (i.e. above LOQ); AUC_{inf}: AUC extrapolated from time of dosing (0) to infinity; AUC_{extrap}: percentage of AUC_{inf} that is due to extrapolation from T_{last} to infinity; Cl: clearance; MRT_{inf}: MRT extrapolated to infinity using the last quantifiable concentration for extrapolation; CL_{tot}/F: total body clearance; Vss/F: volume of distribution at steady state; T_{max}: time of maximum tissue or plasma concentrations; C_{max}: maximum tissue or plasma concentrations. Standard error of the mean (SEM) was estimated for C_{max} and AUC_{last}. (a): not statistically significantly different ($p > 0.05$) between VBPO and DLVBPO. (b): statistically significantly different ($p \leq 0.05$) between VBPO and DLVBPO